

Initial stages of selenium electrodeposition onto glassy carbon electrode

Antanas Steponavičius¹,

Dijana Šimkūnaitė^{1*},

Ignas Valsiūnas¹,

Gintaras Baltrūnas²

¹ *Institute of Chemistry,
Center for Physical Sciences
and Technology,
A. Goštauto 9,
LT-01108 Vilnius, Lithuania*

² *Department of Physical
Chemistry, Vilnius University,
Naugarduko 24,
LT-03325 Vilnius, Lithuania*

Initial stages of selenium electrodeposition onto GC electrode were investigated in the sulphuric acid medium by means of cyclic voltammetry, chronoamperometry and electrochemical impedance spectroscopy. The chronoamperometric results were shown to follow the progressive 3D nucleation and diffusion-controlled growth model by Scharifker and Hills. Electrochemical impedance spectroscopy investigations have revealed that the presence of a thin Se layer on the GC electrode does not change the inhomogeneity of the surface significantly, as the estimated values of the parameter n were very close for the bare GC and Se-modified GC electrodes and equal to ~ 0.9 , but it affects the charge transfer rate at the applied $E = 0.2$ V. The estimated charge transfer resistance values for bare and selenium-covered GC electrodes differ markedly and range from $1872 \Omega \text{ cm}^2$ to $1007 \Omega \text{ cm}^2$, respectively. The obtained parameters of CPE capacitance and the ohmic resistance of the electrolyte solution for bare GC and Se-covered GC electrodes at the potential value $E = 0.2$ V are close and vary slightly, indicating that the structure of the double layer undergoes an insignificant alteration and the additional ohmic drop across the interfacial layer is negligible.

Key words: selenium, electrodeposition, early stages, glassy carbon electrode

INTRODUCTION

The electrodeposition of selenium and metal chalcogenides has received considerable attention not only from the academic point of view but for the large area of their possible applications ranging from the chemical analysis [1, 2] to electrochemical growth of compound semiconductors [3]. Their prominent features such as light sensitivity and good semiconducting properties have made selenium particularly promising in the production of so-called metal selenides (CdSe, ZnSe, PbSe, In₂Se₃, CuInSe₂, etc.). Potential uses of such compounds are highly intriguing in technological applications like optoelectronics, advanced thin film solar cells, IR detectors, solid state lasers, biological sensors, thermoelectric cooling materials, etc. [3–6].

Selenium and selenides can be obtained by a variety of techniques, but electrodeposition is convenient for large area deposition; it is least costly, effective, simple and readily adoptable method when compared with most physical meth-

ods [7, 8]. The cathodic reduction of selenious acid is known to be the best way to obtain Se films in the so-called metallic form (resistivity $1 \Omega \text{ cm}$) [9] or the amorphous insulating form (resistivity $10^5 \Omega \text{ cm}$) [10]. Moreover, Se electrodeposition always occurs as a side reaction in the cathodic synthesis of metal selenides [11].

Considerable work has already been done in investigating the mechanism and kinetics of the H₂SeO₃ reduction/oxidation process in different solutions of various composition [11–20]. This process is rather complicated and complex due to several factors such as the presence of a coupled chemical reaction and the sensitivity of Se(IV) electrochemistry to the substrate surface. Electrodeposition of selenium on different substrates has been presented in [5, 11, 13, 19–26]; however, these studies are mainly based on the reduction pathway for Se(IV) [11, 13, 19, 24, 25], surface structure of Se atom layers [23, 26], characterization of Se films [20, 27], or the analysis of trace amounts of Se [11]. Investigations of the initial stages (nucleation and growth mechanism) of selenium film deposition have remained largely ignored.

* Corresponding author: E-mail: nemezius@ktl.mii.lt

The nucleation and growth are of primary importance as they play a decisive role in film structure and properties [28]. They are usually investigated using foreign substrates, such as platinum, gold and carbon including glassy carbon (GC). Particular studies have been performed applying a GC electrode. The specific properties of this electrode are low cost, good electrical conductivity and high surface quality with excellent polishing characterizations. To the best of our knowledge, the only study on the initial stages of Se electrodeposition onto non-reactive SnO₂ electrodes has been presented in [29]. It has been shown that at low overpotentials, the deposition of Se proceeds by a four-electron reduction of Se(IV) to Se(0) and 2D growth under instantaneous nucleation followed by a multiplayer spiral growth mode. At high overpotentials, the deposition of Se occurs through a comproportionation reaction between Se(IV) and Se(-II) generated from a six-electron reduction of Se(IV) and 3D growth under progressive nucleation.

It is known that in the electrochemical formation of selenides, such as ZnSe, CdSe and CuInSe₂, selenium is generally deposited first. Therefore, the nucleation and growth of the first layer of Se is also the first step in the electrochemical formation of selenides. Moreover, semiconductor nanocrystals exhibit a wide range of shape and size-dependent properties [30, 31]. It is mostly in the regime below 10 nm where this variable comes into play. Variations in fundamental characteristics ranging from phase transitions to electrical conductivity can be induced by controlling the size and shape of the particles. To obtain the desirable quality of selenium and selenide thin films, a closer examination of the nucleation and growth mechanism during selenium electrodeposition is of first importance.

The present work deals with the examination of the early stages of Se nucleation and growth onto GC electrode in the sulphuric acid medium, in which cyclic voltammetry (CV), chronoamperometry (CA) and electrochemical impedance spectroscopy (EIS) were employed.

EXPERIMENTAL

The working solution was 0.5 M H₂SO₄ containing H₂SeO₃ in amounts of 1 to 1.6 mM. It was prepared from triply distilled water, ultra-pure sulphuric acid (Russia) and selenious acid (99.999% purity, Aldrich). Prior to each experiment, the working solution had been deaerated with Ar gas for 0.5 h.

All electrochemical experiments were carried out at 20 ± 1 °C in a conventional three-electrode cell. The working electrode was glassy carbon (GC) (CY-2000) sheet of ca. 1 cm², dressed in glass. The counter-electrode was a Pt sheet of ca. 4 cm² in area, and the reference electrode was Ag / AgCl / KCl (sat.). In the text, all potentials (*E*) were recalculated with respect to the standard hydrogen electrode (SHE), unless otherwise stated.

The pretreatment of the electrode prior to each electrochemical measurement was as follows: (i) mechanical polish-

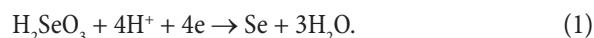
ing to a nearly mirror finish with successively finer grades of alumina powders, eventually to 0.05 μm, and cleaned ultrasonically in sequence in acetone, diluted HCl and triply distilled water; (ii) to obtain a clean reproducible surface before each following measurement, the GC electrode was also scanned in the background 0.5 M H₂SO₄ solution at a potential scan rate 50 mV · s⁻¹ for 20 min between $E_{sc} \approx +0.25$ and $E_{sa} \approx +1.5$ V.

The electrochemical investigations were carried out using the cyclic voltammetry, single potential step and electrochemical impedance spectroscopy techniques. EIS measurements were obtained at a 0.1 to 8 kHz frequency range and the 0.005 V (p / p) amplitude. Cyclic voltammograms (CVs), potentiostatic *I* / *t* curves and EIS spectra were recorded using an μAutolab Type III.

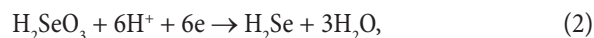
RESULTS AND DISCUSSION

Figure 1 shows the cyclic voltammograms recorded for the GC electrode in 0.5 M H₂SO₄ solution containing increasing amounts of H₂SeO₃ within the anodic limit $E_{sa} = +1.5$ V and cathodic limit $E_{sc} = -0.55$ V. In the case of a solution with a higher concentration of the reactant, two well defined cathodic peaks (labeled C1 and C2) at E_{pc1} about +0.15 V and E_{pc2} about -0.12 V have been revealed (Fig. 1a). In the least concentrated solution, poorly defined waves appear. The curve inbetween the mentioned concentrations displays two cathodic peaks, the second, being followed by an ill-developed peak at a more negative *E* (about -0.17 V). Poorly defined voltammetric curves with a single cathodic peak about -0.80 V vs. SCE of H₂SeO₃ onto GC electrodes in different acid media have been recorded [14]. Results reported in [11, 14] have indicated that the behaviour of H₂SeO₃ depends markedly on the kind and pretreatment modes of the carbon electrodes used.

In the context of works [11, 13, 17, 19, 23–25, 32–34], the cathodic peak C1 at the potential value of about +0.15 V corresponds to bulk selenium deposition through four-electron reduction of Se(0) by Eq. (1):



Another cathodic peak, C2, at more negative potentials ~ -0.12 V is associated with formation of H₂Se species through a direct six-electron reduction of Se(IV) to Se(-II) according to Eq. (2) [11, 21, 29],



or / and Eq (3):



At more positive potentials the process described by Eq. 3, with transference of two electrons, is possible [21, 29].

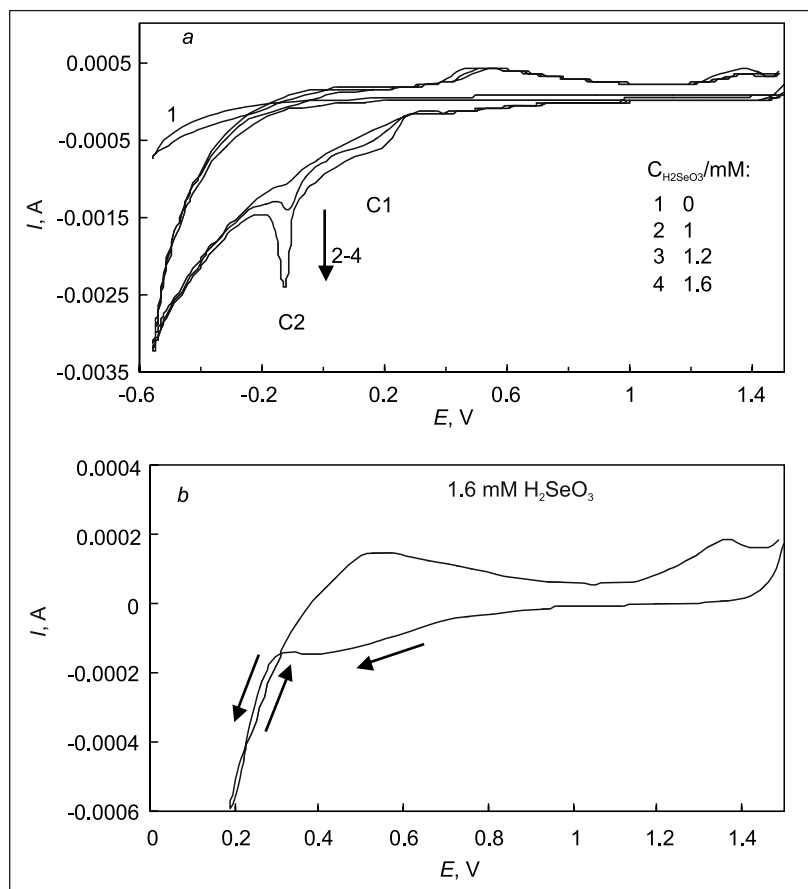


Fig. 1. Cyclic voltammograms for GC electrode in 0.5 M H_2SO_4 solution containing: *a* – increasing amounts of H_2SeO_3 between $E_{sa} = +1.5$ V and $E_{sc} = -0.55$ V, *b* – 1.6 mM H_2SeO_3 between $E_{sa} = +1.5$ V and $E_{sc} = 0.20$ V. Scan rate $\nu = 50$ mV s $^{-1}$

The product Se(–II) then undergoes a comproportionation reaction with Se(IV), leading to the chemical formation of Se(0) [19], which is usually attributed to the amorphous form of selenium:



In (CVs), this reaction can appear along with a process described by Eq. 2 as a single peak or as closely spaced two peaks depending on the sweep rate, upper potential limit and H_2SeO_3 concentration [11, 24]. The similar character of two closely spaced peaks is observed when H_2SeO_3 concentration of 1.2 mM is used (Fig. 1). When the concentration of H_2SeO_3 is high enough, reaction (4) becomes fast, and the overall process according to reactions (2) and (4) looks like a four-electron reduction (Eq. 1) [11].

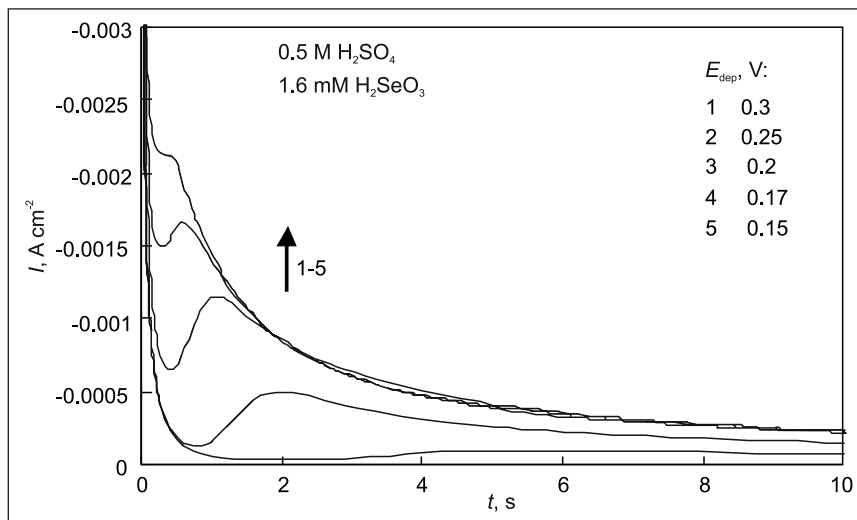
The cyclic voltammogram recorded for the GC electrode in 0.5 M H_2SO_4 solution containing 1.6 mM H_2SeO_3 within the cathodic limit $E_{sc} = 0.20$ V displays a slight initial increase of current before peak C1, followed by a hysteresis loop (Fig. 1b). A similar weak reduction current has been observed in [29, 33, 34]. It is usually assigned to the four-electron selenium predeposition on a foreign substrate before the overpotential deposition of bulk selenium.

The presence of a nucleation loop is diagnostic for the formation of selenium nuclei onto GC electrode and has been found to be indicative of the nucleation / growth process [35].

Generally, these current loops occur because metal deposition onto a foreign substrate during cathodic scan requires a considerable overpotential in order to initiate the nucleation and subsequent growth of a deposit. Then the scan direction is reversed, the reduction faradaic current continues flowing, because the metal deposition now takes place on the nucleated surface of the substrate.

The nucleation process was analysed by the potential step technique. Figure 2 shows a family of potentiostatic I/t transients for various potentials obtained onto GC electrode in 0.5 M $\text{H}_2\text{SO}_4 + 1.6$ mM H_2SeO_3 solution. The shape of these chronoamperograms is typical of a diffusion-limited reaction for the nucleation and growth of a metal deposit onto a foreign substrate [28, 36]. The transients are characterized by a sharp current decline due to a double layer charging, the current exhibiting the induction time attributed to the incubation time for nucleation and a current increase due to the nucleation and growth of isolated nuclei. As the size or / and the number of the nuclei grow, the overlap of spherical diffusion fields gives rise to a current maximum (I_{\max}) at t_{\max} , followed by a decaying current. I_{\max} increases and t_{\max} decreases as the applied deposition potential (E_{dep}) is shifted towards lower values. These features are consistent with the Sharifker and Hills (SH) model for 3D nucleation with diffusion-controlled growth [36]. This model implies the formation and growth of the initial nuclei onto a surface of foreign substrate at $t < t_{\max}$, the overlap of the diffusion zones around them at $t = t_{\max}$ and

Fig. 2. Potentiostatic current transients for Se electrodeposition onto GC electrode in 0.5 M H₂SO₄ + 1.6 mM H₂SeO₃ solution recorded at different deposition potentials E_{dep}



the further growth on the initial layer of the substrate surface at $t > t_{\text{max}}$.

Two limiting cases – instantaneous and progressive nucleation – have been predicted according to SH theory. One of the methods for distinguishing between these two limiting cases is to compare the experimental transients plotted in a non-dimensional plot, $(I/I_{\text{max}})^2$ vs. t/t_{max} , with the theoretical plots calculated for instantaneous (Eq. 5) and progressive (Eq. 6) 3D nucleation with the diffusion-controlled growth process [36]:

$$\left(\frac{I}{I_{\text{max}}}\right)^2 = 1.9542\left(\frac{t}{t_{\text{max}}}\right)^{-1} \{1 - \exp[-1.2564\left(\frac{t}{t_{\text{max}}}\right)]\}^2 \quad (5)$$

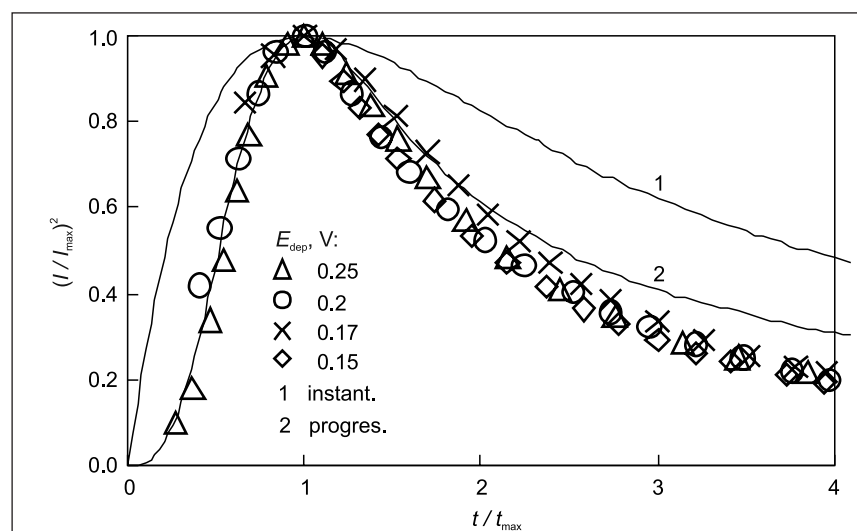
$$\left(\frac{I}{I_{\text{max}}}\right)^2 = 1.2254\left(\frac{t}{t_{\text{max}}}\right)^{-1} \{1 - \exp[-2.3367\left(\frac{t}{t_{\text{max}}}\right)^2]\}^2 \quad (6)$$

To make a comparison convenient, it is necessary to make a correction for the induction time t_0 . It could be obtained from the intercepts of the straight lines of $I^{2/3}$ vs. t [37]. The corrected experimental $(I/I_{\text{max}})^2$ vs. t/t_{max} plots along with the plots calculated from equations (5) and (6) are shown in

Fig. 3. Within the whole E_{dep} region applied, the experimental curves show a rather good correlation with the theoretical curve for progressive nucleation. Only for a longer time ($t \gg t_{\text{max}}$) a negligible negative deviation from the ideal theoretical progressive nucleation is observed. These deviations are often detected [38–43] and can occur for different reasons. Among them, the presence of a reaction parallel to metal deposition or mixed charge transfer and mass transport control are mentioned. In our case, the presence of a reaction parallel to Se deposition can be attributed to the beginning of H₂Se evolution, followed by a chemical reaction according to Eq. 4.

The EIS method has been regarded as an effective and practical method for probing the interfacial features of bare and surface-modified electrodes. In the present paper, only preliminary impedance data are discussed. Figure 4 shows the impedance responses as the Nyquist plot (Z'' vs Z') of the bare GC electrode (curve 1) and Se-covered (~12 ML) GC electrode (curve 2) in 0.5 M H₂SO₄ solution containing 1.6 mM H₂SeO₃ at $E = 0.2$ V. Modification of the GC was performed by the multiple potential step technique in the so-

Fig. 3. Nondimensional plots of potentiostatic current transients recorded onto GC electrode in 0.5 M H₂SO₄ + 1.6 mM H₂SeO₃ solution (data from Fig. 2). Lines, theoretical instantaneous (1) and progressive (2) 3D nucleation and diffusion-controlled growth according to SH model



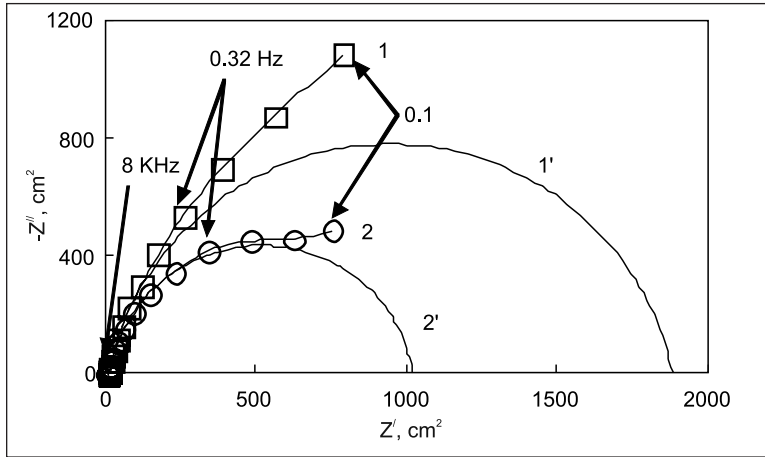


Fig. 4. Nyquist plots for bare GC (1) and Se-covered GC (2) electrodes and simulated semicircles (1' and 2'), respectively, in 0.5 M H_2SO_4 + 1.6 mM H_2SeO_3 solution at the potential $E = 0.2$ V

lution of the same concentrations at $E = 0.2$ V. The electric charge Q_{Se} involved in the Se(IV) reduction and, subsequently, the coverage of the surface with Se layers were evaluated by integrating the profile of $i-t$ transient, assuming that four electrons are exchanged per Se adatom in the surface reduction reaction according to Eq. (1). The impedance spectrum in Fig. 4 includes a semicircle portion corresponding to the charge transfer limited process and implies the features associated with the charge transfer process accompanied by electrosorption of selenium species onto the electrode surface. As the charge transfer resistance (R_{ct}) at the electrode surface is equal to the semicircle diameter of EIS, it can be used to describe the interface properties of the electrode. The fitted semicircle through a part of the measured curves at high frequencies shows a close coincidence with the experimental data, indicating that experimental results could be fitted to the classical Ershler–Randles equivalent circuit (Fig. 5). The circuit includes the following elements: (1) the ohmic resistance of the electrolyte solution (R_s), (2) the charge transfer resistance (R_{ct}), and (3) the double layer capacitance replaced by a constant phase element (CPE) as the roughness of the electrode surface should be taken into account. The double layer of the solid electrode in solution, simulated as CPE with impedance, can be defined as [44]

$$Z_{(CPE)} = A^{-1}(j\omega)^{-n}, \quad (7)$$

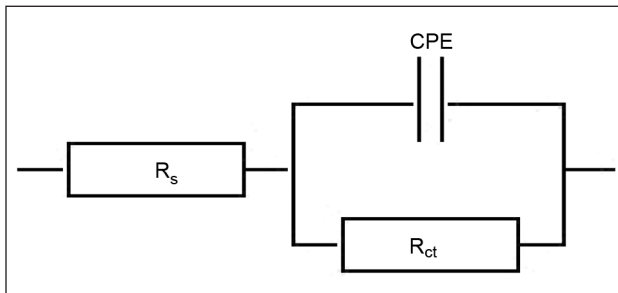


Fig. 5. Equivalent circuit for electrodes shown in Fig. 4: R_s – uncompensated solution resistance, R_{ct} – charge transfer resistance across electrode / solution interface, CPE – constant phase element representing interfacial capacitance

where A and n are frequency-independent parameters ($0 \leq n \leq 1$). Factor A corresponds to the double-layer capacitance, and the exponent n shows the impedance phase shift. When the electrode surface is homogeneous, n is unity and Eq. 7 transforms into the simple double layer capacitance with the impedance

$$Z_{(CPE)} = (C_{dl}j\omega)^{-1}. \quad (8)$$

The deviation of the exponent n from unity is usually small even for a rough metal surface and ranges within 0.9 to 1. However, this deviation may increase drastically when the surface is covered with an inhomogeneous low-conductivity layer [44]. Formation of Se layers onto the GC surface are expected to affect the n values as well as the values of R_s , R_{ct} and CPE capacity significantly in case an amorphous insulating layer is present. The R_{ct} values can be calculated from the difference in the impedance plot at lower and higher frequencies. The C_{CPE} values can be calculated from the following equation [43]:

$$C_{CPE} = (\omega_{max} R_{ct})^{-1}, \quad (9)$$

where ω_{max} is angular frequency at which the imaginary part of the impedance is maximum (Z''_{max}). The calculated values conform well with the values obtained from the simulated plots (Fig. 4), assuming the equivalent circuit with the CPE parallel to the resistance R_{ct} and resistor in series, and are given in Table. Modification of the GC electrode with a thin Se layer results in a decrease of the diameter of the semicircle (Fig. 4) and, consequently, in a significant decrease of R_{ct} down to 1 007 $\Omega \text{ cm}^2$ for the selenium-covered GC electrode

Table. Parameters of equivalent circuit presented in Fig. 5 for EIS response of bare GC and Se-covered GC electrode in 0.5 M H_2SO_4 solution containing 1.6 mM H_2SeO_3 at $E = 0.2$ V

Electrode	$R_s, \Omega \cdot \text{cm}^2$	$R_{ct}, \Omega \cdot \text{cm}^2$	CPE $\mu\text{F} \cdot \text{cm}^{-2}$	n
Bare GC	11.66	1 872	795	0.89
Se-covered GC	14.96	1 007	781	0.90

as compared with the $R_{ct} = 1872 \Omega \text{ cm}^2$ for the bare GC electrode. Such an alteration of the R_{ct} values and a negligible deviation of the exponent n from unity imply that the occurrence of a thin Se layer on the GC electrode does not change the inhomogeneity of the surface significantly, but affects the charge transfer rate markedly. Assuming that Se reduction at $E = 0.2 \text{ V}$ proceeds through the four-electron reaction according to Eq. (1), deposition of Se should be notably facilitated if Se is predeposited on the surface of the GC electrode. So, the Se-covered GC electrode has the features typical of conductive materials and accelerates charge transfer in the conditions under study. The observed deviation of experimental results from the fitted semicircle at low frequencies in Fig. 4 is an evidence of a homogeneous or / and heterogeneous chemical reaction. The crystallization reaction could not be excluded, either.

Noteworthy are also the high values of CPE capacitance ranging from 795 to 781 $\mu\text{F} \cdot \text{cm}^{-2}$. The possible reasons for such a phenomenon may be (a) the adsorption–desorption processes occurring on the electrode surface or / and (b) an increase in the surface area, bearing in mind that the GC electrode was pretreated by cycling in the background 0.5 M H_2SO_4 solution between $E_{sc} \approx +0.25$ and $E_{sa} \approx +1.5 \text{ V}$; anyway, the structure of the double layer undergoes quite insignificant changes if a thin Se layer is present on the surface of the GC electrode.

As demonstrated by data in Table, the value R_s close to 14.96 $\Omega \text{ cm}^2$ for the Se-covered GC electrode is slightly higher than $R_s = 11.66 \Omega \text{ cm}^2$ for the bare GC, indicating the occurrence of a negligible additional ohmic drop across the interfacial layer. An analogous phenomenon was observed for a Se-covered Ti electrode [20]. The increase of R_s values was ascribed to the formation of a resistive film, and the resistivity close to 4000 $\Omega \text{ cm}$ was obtained. The estimated value was intermediate between those reported in the literature for amorphous and hexagonal Se. Following [20], if the increase of R_s is ascribed to the formation of a resistive film, analogous specific resistivity can be obtained from the impedance increase (3.3 $\Omega \text{ cm}^2$) for a Se-covered GC. The estimated value is equal to $0.5 \cdot 10^7 \Omega \text{ cm}$ and could be attributed to the insulating amorphous form of Se. If this is the case, it should be an indication of the occurrence of chemical reaction according to Eq. (4) and the presence of Se(-II) even at the rather positive $E = 0.2 \text{ V}$ value applied. However, the physical meaning of the R_s value is not quite clear as the contributions of the resistances involved in the process are not well separated. The resistance of the electrolyte solution, as well as the resistance of the thin Se layer and of the bare GC electrode should be taken into account. Thus, the obtained value of specific resistivity is rather approximate; it gives only a preliminary picture, and a particular examination is required.

CONCLUSIONS

In this study, the initial stages of selenium electrodeposition onto GC electrode were investigated in a sulphuric acid medium in the presence of H_2SeO_3 . Analysis of the experimental data indicates a progressive 3D nucleation and diffusion-controlled growth of Se nuclei in accordance with the model proposed by Sharifker and Hills for the early stages of metal electrocrystallization onto a foreign substrate.

Analysis of electrochemical impedance spectroscopy data indicates that the presence of a thin Se layer on the GC electrode does not change the inhomogeneity of the surface significantly as the estimated values of the CPE parameter n are very close for the bare GC and Se-modified GC electrodes and are equal to ~ 0.9 , but it affects the charge transfer rate at the applied $E = 0.2 \text{ V}$ value. The estimated charge transfer resistance values for the bare and selenium-covered GC electrodes differ markedly and range from 1872 $\Omega \text{ cm}^2$ to 1007 $\Omega \text{ cm}^2$. If Se is predeposited on the surface of the GC electrode at $E = 0.2 \text{ V}$, Se reduction could be facilitated markedly. The obtained parameters of CPE capacitance and the ohmic resistance of the electrolyte solution for bare and Se-covered GC electrodes are close and vary slightly, indicating that the structure of the double layer undergoes an insignificant alteration and the additional ohmic drop across the interfacial layer is negligible.

Received 7 January 2011

Accepted 18 February 2011

References

1. S. H. Tan, S. P. Kounaves, *Electroanalysis*, **10**, 364, (1998).
2. T. Ferri, P. Sangiorgio, *Analyt. Chem. Acta*, **385**, 337 (1999).
3. R. K. Pandey, S. N. Sahu, S. Chandra, in: *Handbook of Semiconductor Electrodeposition*, Marcel Dekker Inc., New York (1996).
4. H. W. Schok, *Appl. Surf. Sci.*, **92**, 606 (1996).
5. R. Kowalik, K. Fitzner, *J. Electroanal. Chem.*, **633**, 78 (2009).
6. N. S. Yesugade, C. D. Lokhande, C. H. Bhosale, *Thin Solid Films*, **263**, 145 (1995).
7. I. M. Dharmadasa, J. Haig, *J. Electrochem. Soc.*, **153**, G47 (2006).
8. T. S. Olson, P. Atanassov, D. A. Brevnov, *J. Phys. Chem.*, **B109**, 1243 (2005).
9. A. Von Hippel, M. C. Bloom, *J. Chem. Phys.*, **18**, 1243 (1950).
10. A. K. Graham, H. L. Pinkerton, H. J. Boyd, *J. Chem. Soc.*, **106**, 651 (1959).
11. M. S. Kazacos, B. Millar, *J. Electrochem. Soc.*, **127**, 869 (1980).
12. S. Massaccesi, S. Sanchez, J. Vedel, *J. Electroanal. Chem.*, **412**, 95 (1996).
13. R. W. Andrews, D. C. Johnson, *Analyt. Chem.*, **47**, 294 (1975).

14. G. Jerzabek, Z. Kublik, *J. Electroanal. Chem.*, **114**, 165 (1980).
15. G. Jerzabek, Z. Kublik, *Analyt. Chim. Acta*, **143**, 121 (1982).
16. G. Jerzabek, Z. Kublik, *J. Electroanal. Chem.*, **137**, 247 (1982).
17. R. Modolo, M. Traore, O. Vittori, *Electrochim. Acta*, **31**, 859 (1986).
18. J. M. Feliu, R. Gómez, M. J. Llorca, A. Aldaz, *Surf. Sci.*, **289**, 152 (1993).
19. Ch. Wie, N. Myung, K. Rajeshwar, *J. Electroanal. Chem.*, **375**, 109 (1994).
20. S. Cattarin, F. Furlanetto, M. M. Musiani, *J. Electroanal. Chem.*, **415**, 123 (1996).
21. M. O. Solaliendres, A. Manzoli, G. R. Salazar-Banda, K. I. B. Eguiluz, S. T. Tanimoto, S. A. S. Machado, *J. Solid State Electrochem.*, **12**, 679 (2008).
22. M. F. Cabral, V. A. Pedrosa, S. A. S. Machado, *Electrochim. Acta*, **55**, 1184 (2010).
23. B. M. Huang, T. E. Lister, J. L. Stickney, *Surf. Sci.*, **392**, 27 (1997).
24. M. Alanyalioglu, U. Demir, C. Shanon, *J. Electroanal. Chem.*, **561**, 21 (2004).
25. M. C. Santos, S. A. S. Machado, *J. Electroanal. Chem.*, **567**, 203 (2004).
26. M. Cavallini, G. Aloisi, R. Guidelli, *Langmuir*, **15**, 2993 (1999).
27. S. Z. El Abedin, A. Y. Saad, H. K. Farag, N. Borisenko, Q. X. Liu, F. Endres, *Electrochim. Acta*, **52**, 2746 (2007).
28. E. Budevski, G. Staikov, W. J. Lorenz, in: *Electrochemical Phase Formation and Growth*, VCH, Weinheim, New York, Basel, Cambridge, Tokyo (1996).
29. Y. Lai, F. Liu, J. Li, Y. Liu, *J. Electroanal. Chem.*, **639**, 187 (2010).
30. A. P. Alivisatos, *J. Phys. Chem.*, **100**, 13226 (1996).
31. Y. Badr, M. A. Mahmoud, *Physica B*, **369**, 278 (2005).
32. P. Zuman, G. Somer, *Talanta*, **51**, 645 (2000).
33. M. Kemell, H. Saloniemi, M. Ritala, M. Leskela, *Electrochim. Acta*, **45**, 3737 (2000).
34. T. A. Soreson, T. E. Lister, B. M. Huang, J. Stickney, *J. Electrochem. Soc.*, **146**, 1019 (1999).
35. S. Fletcher, *Electrochim. Acta*, **28**, 917 (1983).
36. B. Sharifker, G. Hills, *Electrochim. Acta*, **28**, 879 (1983).
37. P. M. Rigano, C. Mayer, T. Chierchie, *J. Electroanal. Chem.*, **248**, 219 (1988).
38. R. Schrebler, P. Cury, M. Orellana, H. Gómez, R. Cordova, E. A. Dalchiale, *Electrochim. Acta*, **46**, 4309 (2001).
39. D. Grujicic, B. Pesic, *Electrochim. Acta*, **47**, 2901 (2002).
40. D. Grujicic, B. Pesic, *Electrochim. Acta*, **50**, 4405 (2005).
41. G. Oskam, P. Searson, *J. Electrochem. Soc.*, **147**, 21919 (2000).
42. G. Oskam, P. Searson, *Surface Science*, **446**, 103 (2000).
43. P. V. Dudin, P. R. Unwin, J. Macpherson, *J. Phys. Chem.*, **C114**, 13241 (2010).
44. Z. B. Stoynov, B. M. Grafov, B. S. Savova-Stoinov et al., *Electrochemical Impedance*, Nauka, Moscow (1991).

Antanas Steponavičius, Dijana Šimkūnaitė, Ignas Valsiūnas,
Gintaras Baltrūnas

SELENO ELEKTROLITINIO NUSODINIMO PIRMOSIOS STADIJOS ANT STIKLIŠKOSIOS ANGLIES ELEKTRODO

S a n t r a u k a

Seleno elektrolitinio nusodinimo pirmosios stadijos ant stikliškios anglies (SA) elektrodo buvo tirtos taikant ciklinės voltametrijos, chronoamperometrijos ir elektrocheminio impedanso spektroskopijos metodus sieros rūgšties tirpaluose. Chronoamperometrinių tyrimų rezultatai parodė, kad selenas ant SA nusodinamas pagal Scharifkerio ir Hillso pasiūlytą momentinės 3D nukleacijos ir difuzijos kontroliuojamo augimo mechanizmą. Elektrocheminio impedanso spektroskopijos tyrimai parodė, kad plonas Se sluoksnis ant SA elektrodo paviršiaus itin nekeičia paviršiaus nehomogeniškumo, kadangi nustatytos parametro n reikšmės švaraus SA ir Se padengto SA elektrodų atvejais buvo artimos ir lygios $\sim 0,9$, tačiau turi įtakos krūvio pernešimo greičiui, kai $E = 0,2$ V. Apskaičiuotosios krūvio pernešimo varžos vertės švaram SA ir Se padengtam SA elektrodams labai skiriasi ir kinta atitinkamai nuo 1872 iki 1007 Ω cm². Abiem atvejais CPE talpos ir ominės elektrolito varžos parametrai, kai $E = 0,2$ V, yra artimi ir kinta nežymiai, t. y. dvigubo sluoksnio struktūros pokyčiai tik nereikšmingi ir papildomas ominis kritimas per fazinį sluoksnį nežymus.